TECNIACUSTICA VALENCIA · 2015

46º CONGRESO ESPAÑOL DE ACÚSTICA
ENCUENTRO IBÉRICO DE ACÚSTICA
EUROPEAN SYMPOSIUM ON VIRTUAL ACOUSTICS AND AMBISONICS

UNCERTAINTIES IN ROOM SIMULATIONS

PACS: 43.55.Ka

Vorländer, Michael; Guski, Martin
Institute of Technical Acoustics, RWTH Aachen University, Kopernikusstr. 5, 52074 Aachen, Germany
mvo@akustik.rwth-aachen.de

ABSTRACT

Room simulation requires input data of the room model and the boundary conditions. Uncertainties caused by user-dependent choices have been investigated in previous work. In this paper the influence of specific settings in the algorithmic details such as the number of rays or the temporal resolution, etc. will be studied by calculating energy room impulse response under the condition of variation of such settings. The statistics of the input variables and corresponding output standard deviations concerning room acoustics parameters (reverberation time, strength, clarity, etc.) will be presented, and possible guidelines for robust usage of algorithms will be discussed.

RESÚMEN

Simulación de acústica de salas requiere como datos de entrada el modelo de la sala y las condiciones de contorno. Las incertidumbres causadas por las decisiones que dependen del usuario se han investigado en trabajos anteriores. En este trabajo la influencia de la configuración específica en los detalles algorítmicos tales como el número de rayos o la resolución temporal, etc., serán estudiados calculando la energía de la respuesta al impulso de la sala bajo la condición de variación de tales configuraciones. Se presentarán las estadísticas de las variables de entrada y las correspondientes desviaciones estándar como variables de salida relativas a los parámetros de acústica de la sala (tiempo de reverberación, fuerza, claridad, etc.), y se discutirán las posibles directrices para el uso de algoritmos robustos.

1. INTRODUCTION

Room acoustic simulations are usually based on models of geometrical acoustics such as image sources and ray tracing (Vorländer 2008). Many activities in research and development were reported in publications, and they basically focus on the problem of simulating the important early reflections in the room impulse response (Savioja and Svensson 2015). For the later part, the “diffuse reverberation tail” several alternatives exist, which span from simple stochastic diffuse decay processing to full ray tracing or radiosity. In between, often a mixing time or transition time is suggested to switch from one algorithm to the next (Jeong et al. 2010).

What is not known generally is the dependence of details in the late response on settings in ray tracing. This might introduce differences of results from repeated simulations with the same settings by just changing one parameter at a time, for example the receiver radius, the size of the temporal bins, the number of rays, etc.

In this contribution it is studied how theoretically predicted uncertainties compare with results from computer experiments.

2. FUNDAMENTALS – STATE OF THE ART

Differences in results from simulations with geometrical acoustics are caused by the choice of basic setting such as the transition time, the number of rays, the temporal and spatial resolution of the receiver. Also, these software parameters influence the computation time and are thus of interest if compromises between accuracy and effort must be found.

2.1. Fundamentals of Ray Tracing

There are two variants of ray tracing, which are often confused by users (Vorländer 2013). One (classical ray tracing) is used as a Monte Carlo approach, where the sound energy is distributed into space via rays (or particles) and later collected as temporal series of events in volume detectors. This method allows for inclusion of surface scattering and it directly delivers an impulse response in the time bins recorded at the receiver.

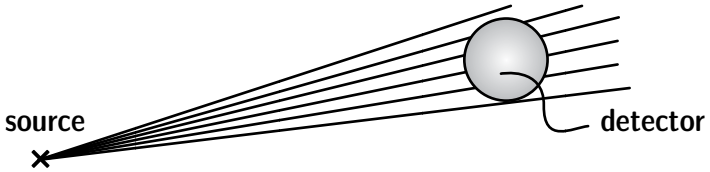

Figure 1: The principle of stochastic ray tracing. The energy-distance law ($1/r^2$) is alredy built-in by counting the rays hitting the receiver sphere.

The other (hybrid ray tracing – image source method) is used to identify paths of specular reflections by shooting rays (or beams, pyramids) in order to find image sources. The impulse response is created in post processing by analysis of the reflections paths, taking into account the spherical wave spread, the wall absorption, etc. This method cannot deall with scattering at all.

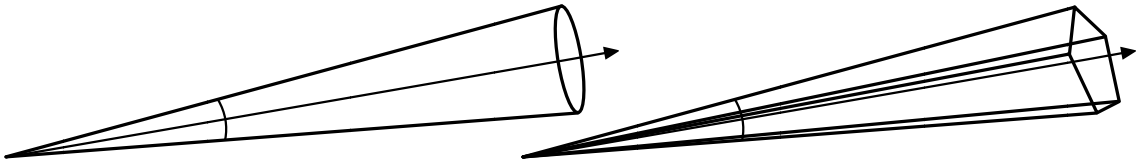

Figure 2: The principle of hybrid ray tracing. The energy-distance law ($1/r^2$) is introduced analytically by using the distance between the source and the receiver.

In both cases, the minimal required number of rays, $N_{\min}$, that is needed to resolve the cone of visibility for a spherical receiver with radius r_d up to time t, is given by

$$N_{min} = \frac{4(ct)^2}{r_d^2} \qquad (1)$$

c denotes the speed of sound.

In the second algorithm (reflection path analysis), this equation is crucial as it determines the lower limit of computation time. In the first algorithm (Monte Carlo ray tracing) it determines no hard limit but a certain probability limit. In the next chapter this aspect is further investigated.

2.2. Uncertainty analysis of ray tracing results (classical method)

In a room the rays are reflected and scattered, and the late decay is created from counting of rays hitting a receiver. This can be done in time bins, or in general terms collecting the total energy, or the immission level. A typical result is depicted in fig. 3. For stochastic ray tracing, which is used for estimation of reverberation tails, a diffuse field of rays (particles) could be assumed. The rays ("counting events") coincide in temporal bins, depending on the specific

algorithms and parameters chosen in the program for detection and absorption. Note that this concept is identical with the concept of particles in a Geiger counter in particle physics.

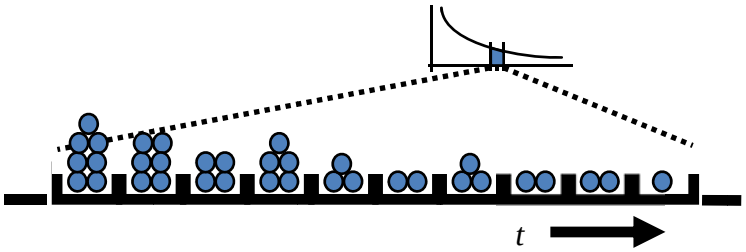

Figure 3: Counted events of rays hitting the receiver, recorded in time bins in the impulse response.

In this case a Poisson distribution can be used to estimate the counting rate, k, of events within a time bin Δt.

$$P(k) = \frac{\langle k \rangle}{k!} e^{-\langle k \rangle} \tag{2}$$

The variance of a Poisson distribution, σ_k, is the identical with the expectation value, $\langle k \rangle$:

$$\sigma_k^2 = \langle k \rangle \tag{3}$$

or expressed by the relative standard deviation

$$\sigma_k / \langle k \rangle = \frac{1}{\sqrt{\langle k \rangle}} \tag{4}$$

For example, if 100 events are counted in one time bin, the standard deviation is 0.1 (10%), in case of 10,000 events, the standard deviation is 0.01 (1%).

If the ray detection event is interpreted as corresponding to sound energy, or sound level, eq. (4) reads:

$$\sigma_{ETC}(t) = 4.34\, \sigma_k / \langle k \rangle \quad \text{dB} \tag{5}$$

In actual simulations, k can be determined at runtime. This will be used in the next chapter in computer experiments. The expectation value, however, can also be calculated with the assumption of a diffuse field, in which N rays are started at the source. Then holds

$$\sigma_{ETC} = 4.34 \sqrt{\frac{V}{N \pi r_d^2 c \Delta t}} \quad \text{dB} \tag{6}$$

which is actually independent of the running time, t, in the impulse response, see fig. 4.

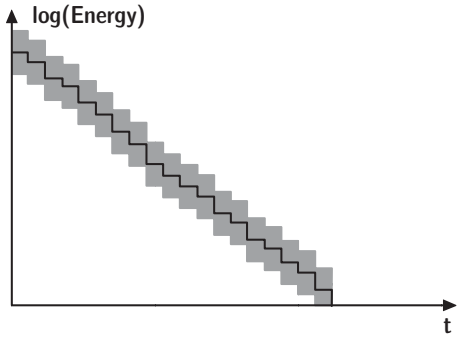

Figure 4: Estimated standard deviation (grey area) in the impulse response around the expectation value (black line).

Moreover, the total energy in the impulse response and correspondingly the parameters sound strength, G, and clarity, C_{80}, are uncertain with a standard deviation of

$$\sigma_G = 4.34\sqrt{\frac{A}{8\pi N r_d^2}} \tag{7}$$

with N the number of rays used and A the equivalent absorption area (according to Sabine's $A = 0.16\,V/T$). Depending on the choice of accuracy the required number of rays can be chosen so that a sufficient repeatability of the runs of the software is ensured. Obviously this depends on the room (on A). Small rooms with $A = 10\,\mathrm{m}^2$ require hardly 8 rays for G or C_{80} to be uncertain to not more than 1 dB, whereas large rooms with $A = 1{,}000\,\mathrm{m}^2$ require 750 rays. Here, it was chosen $r_d = 1\,\mathrm{m}$.

Going back to eq. (6) and discussing the uncertainties in the impulse response, it can be also set a demand on a maximum deviation, say 1 dB again, in the impulse response. The required number of rays for a room volume of 100 m^3 is then 1,760, and for a large room with $V = 10{,}000\,\mathrm{m}^3$, the required N is 176,000. In these examples it is used Δt = 1 ms and r_d = 1 m. The equations re-arranged for the required N read

$$N > \frac{4.34^2}{{\sigma_{ETC}}^2}\frac{V}{\pi r_d^2 c \Delta t} < 17.6\ V/\mathrm{m}^3 \tag{8}$$

and

$$N > \frac{4.34^2}{{\sigma_G}^2}\frac{A}{8\pi r_d^2} \approx 0.75\ A/\mathrm{m}^2 \tag{9}$$

The latter terms are valid for $\sigma = 1\,\mathrm{dB}$, $\Delta t = 1\,\mathrm{ms}$, and $r_d = 1\,\mathrm{m}$.

In the next chapter computer experiments are described and the results discussed in comparison with the predicted standard deviations.

3. COMPUTER EXPERIMENTS

The software RAVEN is used (Pelzer et al. 2014). It consists of a combination of image source algorithms for the early specular part and ray tracing for the scattered and late specular part. It should be noted that RAVEN does not require a transition time but only a maximum image source order. The transition is intrinsically arranged by the scattering effects, which actually start at the first-order reflections.

The standard deviation in the late response is studied in dependence on the radius of the receiver, on the size of the time bins, and on the number of rays. The results are compared by observation of the sound energy, in dB, in the time bins, thus, in the energy time curve. Furthermore, the parameters strength and clarity are investigated.

For the experimental uncertainty analysis the image sources are deactivated, since the deterministic nature will not contribute to the statistical analysis. Two simple shoebox rooms with uniform material properties on all walls are taken as example. The walls have absorption coefficients of 0.2 and scattering coefficients of 1.0. One is a smaller room with volume of 293 m^3 (11m x 9 m x 3m). The source position is p_s = (9.5, 3.5, 1.7) and 12 receivers are spread over the whole room. Another room is larger with a volume of 5525 m^3 (25m x 17m x13 m). The source is positioned at p_s = (4, 7, 3) and 90 receivers are positioned in the room.

In Figure 5 it is shown the standard deviation of the energy of one single time bin at 40 ms in the first part of the impulse response. This refers to the example of the large room. The results are compared between theory (eq. 6) and simulation. The simulations were repeated 5000

times and the relative standard deviation of the sound energies in that time slot was calculated. This result agrees very well with the predicted value.

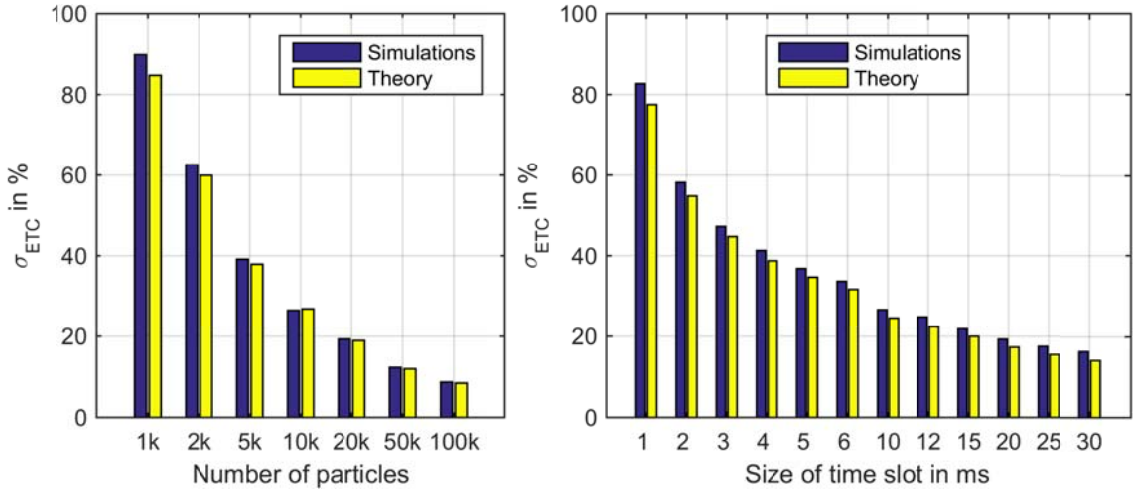

Figure 5: Relative standard deviation of energy in one time bin as function of the number of particles N (left) and the size of time slot Δt (right). It can be seen that simulation and theory match very well.

In figure 6 the time slots size and the receriver sizes are set to 25 ms and 0.6 m, respectively. For the two rooms the relative standard deviation is predicted (solid lines) and evaluated from the computer experiment in 5000 repetitions (broken lines).

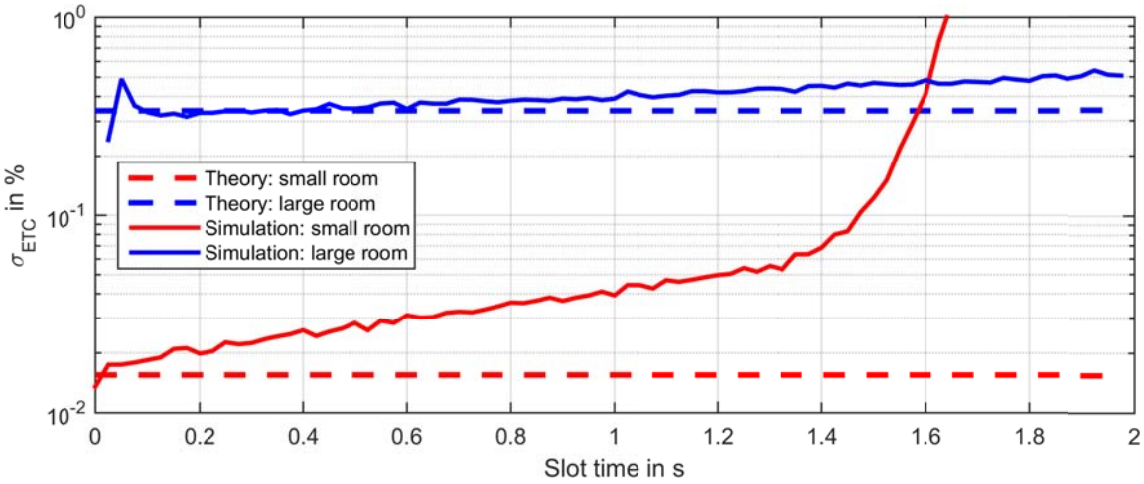

Figure 6: Relative standard deviation of the energy in the time slots as a function of time in the impulse response.

Figure 6 shows interesting features. For the large room (blue) the predicted standard deviation seems to match very well with the result from the computer experiment. There is a linear increase in the result of the computer experiment, however, which indicates a certain loss of rays. This interpretation is based on the trivial fact that the uncertainty increases with smaller numbers of rays. The same phenomenon is visible for the small room but with a steep increase at 1.5 s. A very interesting point in this discussion is that the loop termination in the software is not implemented as a time limit but as a minimum energy limit. The loop is stopped if a ray has suffered an energy loss larger than 130 dB, in fact this occurs on average at 1.5 s for the small room. The 130 dB level loss does not happen at about the same time for all rays paths but in more temporally distributed way, thus indicating a certain distribution of free paths. Some of the rays lose their energy more rapidly because the hit walls more often in time than others.

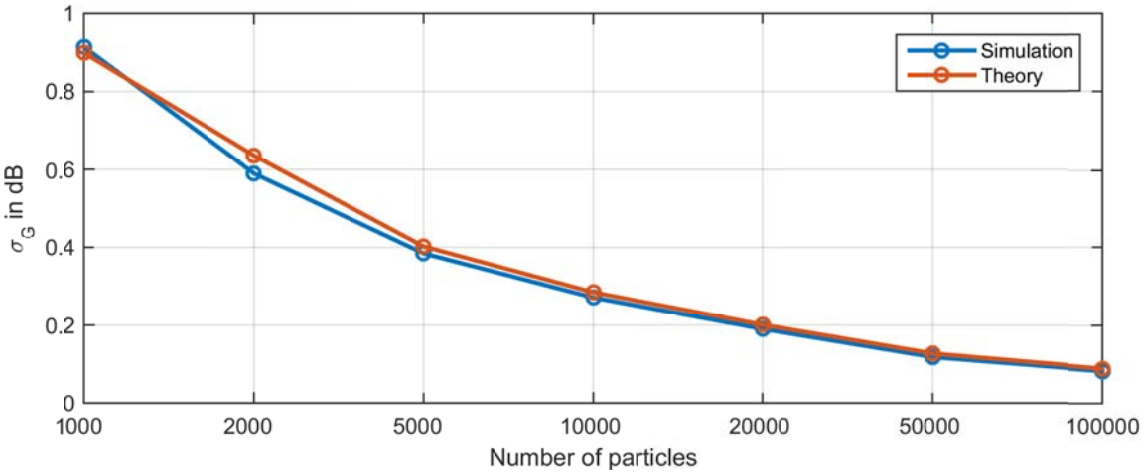

Figure 7: Deviation of sound strength σ_G as function of the number of particles N.

Finally, figure 7 illustrates a very good match of the predicted standard deviation of the sound level (strength *G*, eq. 7) and the results from the computer experiment (1000 repetitions) in dependence on the number of rays.

4. CONCLUSION

Uncertainties can well be predicted for stochastic ray tracing. Using these equations, the required number of rays can be determined for an uncertainty limit of choice. Some results give also insight into the ray distribution as concerns the spatial and temporal ray history. The room shape and size has an impact on the specific free paths, whereas the uncertainty theory just involves the mean free path as one common value. There were exponentially increasing deviations from the predicted uncertainties. One interpretation is that according to the central theorem of statistics a Gaussian free path distribution holds for multiple reflections. The left branch of this distribution contains path lengths shorter than the mean value with a probability that the ray loses energy faster and thus reaches the energy limit earlier. Possibly it is advantageous to implement a time limit rather than an energy limit in the ray tracing algorithm. This observation and interpretation will have to be examined further in the progress of this investigation.

REFERENCES

Jeong, C-H, Brunskog, J, Jacobsen F (2010) Room acoustic transition time based on reflection overlap. J. Acoust. Soc. Am. 127, 2733.

Pelzer, S, Aspöck, L, Schröder, D, Vorländer, M (2014) Interactive Real-Time Simulation and Auralization for Modifiable Rooms. Building Acoustics 21, 65.

Savioja, L, Svensson, UP (2015) Overview of geometrical room acoustic modeling techniques. J. Acoust. Soc. Am. 138, 708.

Vorländer M (2008) Auralization - Fundamentals of acoustics, modelling, simulation, algorithms and acoustic virtual reality. Springer-Verlag, Berlin.

Vorländer M (2013) Computer simulations in room acoustics – concepts and uncertainties. J. Acoust. Soc. Am. 133, 1203.